

This discussion paper is/has been under review for the journal Atmospheric Chemistry and Physics (ACP). Please refer to the corresponding final paper in ACP if available.

# Estimating ground-level PM<sub>2.5</sub> in Eastern China using aerosol optical depth determined from the GOCE Satellite Instrument

J. Xu<sup>1</sup>, R. V. Martin<sup>1,2</sup>, A. van Donkelaar<sup>1</sup>, J. Kim<sup>3</sup>, M. Choi<sup>3</sup>, Q. Zhang<sup>4,5</sup>,  
G. Geng<sup>4,5</sup>, Y. Liu<sup>6</sup>, Z. Ma<sup>6,7</sup>, L. Huang<sup>7</sup>, Y. Wang<sup>4,8,9</sup>, H. Chen<sup>10</sup>, H. Che<sup>11</sup>,  
P. Lin<sup>12</sup>, and N. Lin<sup>13</sup>

<sup>1</sup>Department of Physics and Atmospheric Science, Dalhousie University, Canada

<sup>2</sup>Harvard-Smithsonian Center for Astrophysics, Cambridge, MA, USA

<sup>3</sup>Department of Physics and Atmospheric Sciences, Yonsei University, Seoul, South Korea

<sup>4</sup>Ministry of Education Key Laboratory for Earth System Modeling, Center for Earth System Science, Institute for Global Change Studies, Tsinghua University, Beijing, China

<sup>5</sup>State Key Joint Laboratory of Environment Simulation and Pollution Control, School of Environment, Tsinghua University, Beijing, China

<sup>6</sup>Department of Environmental Health, Rollins School of Public Health, Emory University, Atlanta, GA, USA

<sup>7</sup>State Key Laboratory of Pollution Control and Resource Reuse, School of the Environment, Nanjing University, China

ACPD

15, 17251–17281, 2015

Estimating  
ground-level PM<sub>2.5</sub> in  
Eastern China

J. Xu et al.

[Title Page](#)

[Abstract](#)

[Introduction](#)

[Conclusions](#)

[References](#)

[Tables](#)

[Figures](#)

[◀](#)

[▶](#)

[◀](#)

[▶](#)

[Back](#)

[Close](#)

[Full Screen / Esc](#)

[Printer-friendly Version](#)

[Interactive Discussion](#)



<sup>8</sup>Department of Marine Sciences, Texas A&M University at Galveston, Galveston, TX, USA

<sup>9</sup>Department of Atmospheric Sciences, Texas A&M University, College Station, TX, USA

<sup>10</sup>Institute of Atmospheric Physics, Chinese Academy of Sciences, China

<sup>11</sup>Institute of Atmospheric Composition, Chinese Academy of Meteorological Sciences, China

<sup>12</sup>Department of Atmospheric Sciences, National Taiwan University, Taiwan

<sup>13</sup>Department of Atmospheric Sciences, National Central University, Taiwan

Received: 01 May 2015 – Accepted: 01 June 2015 – Published: 24 June 2015

Correspondence to: J. Xu (junwei.xu@.dal.ca)

Published by Copernicus Publications on behalf of the European Geosciences Union.

[Title Page](#)

[Abstract](#)

[Introduction](#)

[Conclusions](#)

[References](#)

[Tables](#)

[Figures](#)

[|◀](#)

[▶|](#)

[◀](#)

[▶](#)

[Back](#)

[Close](#)

[Full Screen / Esc](#)

[Printer-friendly Version](#)

[Interactive Discussion](#)



## Abstract

We determine and interpret fine particulate matter ( $PM_{2.5}$ ) concentrations in East China for January to December 2013 at a horizontal resolution of 6 km from aerosol optical depth (AOD) retrieved from the Korean Geostationary Ocean Color Imager (GOCI)

5 satellite instrument. We implement a set of filters to minimize cloud contamination in GOCI AOD. Evaluation of filtered GOCI AOD with AOD from the Aerosol Robotic Network (AERONET) indicates significant agreement with mean fractional bias (MFB) in Beijing of 6.7 % and northern Taiwan of –1.2 %. We use a global chemical transport model (GEOS-Chem) to relate the total column AOD to the near-surface  $PM_{2.5}$ .

10 The simulated  $PM_{2.5}$ /AOD ratio exhibits high consistency with ground-based measurements (MFB = –0.52–8.0 %). We evaluate the satellite-derived  $PM_{2.5}$  vs. the ground-level  $PM_{2.5}$  in 2013 measured by the China Environmental Monitoring Center. Significant agreement is found between GOCI-derived  $PM_{2.5}$  and in-situ observations in both annual averages ( $r = 0.81$ ,  $N = 494$ ) and monthly averages (MFB = 13.1 %), indicating

15 GOCI provides valuable data for air quality studies in Northeast Asia. The GEOS-Chem simulated chemical speciation of GOCI-derived  $PM_{2.5}$  reveals that secondary inorganics ( $SO_4^{2-}$ ,  $NO_3^-$ ,  $NH_4^+$ ) and organic matter are the most significant components. Biofuel emissions in northern China for heating are responsible for an increase in the concentration of organic matter in winter. The population-weighted GOCI-derived  $PM_{2.5}$  over

20 East China for 2013 is  $53.8 \mu\text{g m}^{-3}$ , threatening the health and life expectancy of its 600 million residents.

## 1 Introduction

Fine particulate matter with aerodynamic diameter less than  $2.5 \mu\text{m}$  ( $PM_{2.5}$ ) is a robust indicator of mortality and other negative health effects associated with ambient air pollution (Goldberg et al., 2008; Laden et al., 2006). It is estimated that more than three million people lost their lives prematurely due to  $PM_{2.5}$  in 2010 (Lim et al., 2012),

ACPD

15, 17251–17281, 2015

## Estimating ground-level $PM_{2.5}$ in Eastern China

J. Xu et al.

[Title Page](#)

[Abstract](#)

[Introduction](#)

[Conclusions](#)

[References](#)

[Tables](#)

[Figures](#)

◀

▶

◀

▶

[Back](#)

[Close](#)

[Full Screen / Esc](#)

[Printer-friendly Version](#)

[Interactive Discussion](#)



of which one million occurred in East Asia (Silva et al., 2013). In China, there have already been several episodes with  $PM_{2.5}$  described as “beyond index” levels. Thus, it is of paramount importance to monitor  $PM_{2.5}$  concentration across China. Satellite remote sensing is emerging as a key solution to the need of monitoring  $PM_{2.5}$ .

5 Satellite retrievals of aerosol optical depth (AOD), which provide a measure of the amount of light extinction through the atmospheric column due to the presence of aerosols, have long been recognized to relate to ground level  $PM_{2.5}$  (Wang and Christopher, 2003). Many studies have developed advanced statistical relationships between satellite AOD and surface  $PM_{2.5}$ , and have successfully estimated surface  $PM_{2.5}$  with 10 high accuracy (Liu et al., 2009; Kloog et al., 2012; Hu et al., 2013). For example, Ma et al. (2014) estimated  $PM_{2.5}$  concentrations in China from satellite AOD by developing a national-scale geographically weighted regression model, and found significant agreement ( $R^2 = 0.64$ ) with ground measurements.

In addition to empirical statistical methods, satellite AOD can also be geophysically 15 related to surface  $PM_{2.5}$  by the use of a chemical transport model to simulate the  $PM_{2.5}$  to AOD relationship (Liu et al., 2004; van Donkelaar et al., 2010). This approach was first demonstrated using data from the Multiangle Imaging Spectroradiometer (MISR) aboard NASA’s Terra satellite over the United States for 2001 (Liu et al., 2004). Van 20 Donkelaar et al. (2006, 2010) extended this approach to estimate  $PM_{2.5}$  from AOD retrieved from both the MODIS (Moderate Resolution Imaging Spectroradiometer) and the MISR satellite instruments, and developed a long-term global estimate of  $PM_{2.5}$  at a spatial resolution of approximately  $10\text{ km} \times 10\text{ km}$ . Boys et al. (2014) used AOD retrieved from MISR and the SeaWiFS (Sea-viewing Wide Field-of-view Sensor) to produce a 15 year (1998–2012) global trend of ground-level  $PM_{2.5}$ . These previous 25 studies have proven to be globally effective, but more detailed investigation is needed in the most polluted and populated regions like China.

In this study, we estimate the ground-level  $PM_{2.5}$  in eastern China for 2013 at a horizontal resolution of  $6\text{ km}$ , by using AOD retrieved from the Geostationary Ocean Color Imager (GOCl), coupled with the relationship of  $PM_{2.5}$  to AOD simulated by

[Title Page](#)[Abstract](#)[Introduction](#)[Conclusions](#)[References](#)[Tables](#)[Figures](#)[|◀](#)[▶|](#)[◀](#)[▶](#)[Back](#)[Close](#)[Full Screen / Esc](#)[Printer-friendly Version](#)[Interactive Discussion](#)

a chemical transport model (GEOS-Chem). Section 2 describes the approach and data used in this study. Section 3 evaluates the GOCI AOD, the simulated  $PM_{2.5}$  to AOD relationship, and the annual and monthly GOCI-derived  $PM_{2.5}$  using recently available ground-level measurements from the China Environmental Monitoring Center 5 (<http://113.108.142:20035/emcpublish/>). We also interpret the GOCI-derived  $PM_{2.5}$  by using the GEOS-Chem model to estimate its chemical speciation. Section 4 summarizes the major findings and potential future improvements to the current analysis.

## 2 Methods

### 2.1 Aerosol optical depth from the GOCI satellite instrument

10 GOCI is the first geostationary instrument that offers multi-spectral aerosol optical properties in Northeast Asia. GOCI operates onboard the Communication, Ocean, and Meteorology Satellite (COMS) that was launched in 2010 in Korea (Lee et al., 2010). The spatial coverage of GOCI is 2500 km  $\times$  2500 km in Northeast Asia, including eastern China, the Korean peninsula and Japan (Kang et al., 2006). GOCI has eight spectral 15 channels for aerosol retrievals, including six visible bands at 412, 443, 490, 555, 660, 680 nm and two near infrared bands at 745 and 865 nm (Park et al., 2014). The Level 2 AOD products are retrieved at a spatial resolution of 6 km, using a clear-sky composite method for surface reflectance and a lookup table approach based on AERONET observations (Lee et al., 2010, 2012). From its geostationary platform, GOCI has the 20 capacity to provide hourly aerosol optical properties from 09:00 to 16:00 Korean Standard Time (Park et al., 2014), which exceeds the retrieval density of traditional low earth orbiting satellite instruments by a factor of about 8.

A challenge using GOCI to detect aerosols in the atmosphere is the absence of mid-infrared (IR) channels to detect clouds, which means that significant errors could be induced in the estimates of AOD. The operational GOCI products screen clouds based 25 on spatial variability and threshold tests at each 6 km  $\times$  6 km pixel in combination with

[Title Page](#)

[Abstract](#)

[Introduction](#)

[Conclusions](#)

[References](#)

[Tables](#)

[Figures](#)

◀

▶

◀

▶

[Back](#)

[Close](#)

[Full Screen / Esc](#)

[Printer-friendly Version](#)

[Interactive Discussion](#)



a meteorological imager that has 4 IR channels (at 3.7, 6.7, 10.8, 12  $\mu\text{m}$  wavelengths) at 4 km resolution onboard the same satellite (Cho et al., 2006). However, as will be shown here cloud contamination still occurs. Therefore, we apply a set of spatial filters following Hyer et al. (2011) and temporal filters to further eliminate cloud contamination in GOCI AOD. The filters include (1) setting a minimum number of 15 retrievals per 30 km  $\times$  30 km grid cell, (2) using a local variance check to eliminate grid cells where the coefficient of variation (standard deviation/mean) of AOD is larger than 0.5 within the grid cell and (3) excluding grid cells with diurnal variation (maximum–minimum) of AOD larger than 0.74 which is the 90th percentile of diurnal variation of AERONET AOD in Beijing and northern Taiwan for 2013. In this study, we use GOCI AOD for January–December 2013 to derive ground-level  $\text{PM}_{2.5}$  in eastern China.

## 2.2 Aerosol optical depth from AERONET ground-based measurements

The Aerosol Robotic Network (AERONET) is a globally distributed network of CIMEL Sun photometers (Holben et al., 1998) that provide multi-wavelength AOD measurements with a low uncertainty of  $< 0.02$  (Holben et al., 2001). We use All-Points AERONET Level 1.5 cloud screened (Smirnov et al., 2000) data for January–December 2013 from 4 stations within the GOCI domain: Beijing, Beijing-CAMS, Taipei\_CWB and EPA-NCU. Criteria for selecting an AERONET station are (1) a  $\text{PM}_{2.5}$  ground monitor has to be located within 10 km and (2) a complete time series of AOD data records for the period of study has to be available. The Beijing and Beijing-CAMS stations are located in downtown Beijing, with the closest available  $\text{PM}_{2.5}$  monitors 9.5 and 7.5 km away, respectively. Due to the small number of  $\text{PM}_{2.5}$  records at each station, we combine the AERONET AOD from the Beijing and Beijing-CAMS stations and  $\text{PM}_{2.5}$  from the corresponding two ground-based sites as “combined Beijing” site. Taipei\_CWB and EPA-NCU are located in populated northern Taiwan, with nearly collocated  $\text{PM}_{2.5}$  monitors ( $< 3$  km). We similarly combine the Taipei\_CWB and EPA-NCU as “northern Taiwan” site. We use these sites to evaluate GOCI AOD and the relationship between AOD and  $\text{PM}_{2.5}$  simulated by a global chemical transport model.

<a href="#">Title Page</a>	
<a href="#">Abstract</a>	<a href="#">Introduction</a>
<a href="#">Conclusions</a>	<a href="#">References</a>
<a href="#">Tables</a>	<a href="#">Figures</a>
<a href="#">◀</a>	<a href="#">▶</a>
<a href="#">◀</a>	<a href="#">▶</a>
<a href="#">Back</a>	<a href="#">Close</a>
<a href="#">Full Screen / Esc</a>	
<a href="#">Printer-friendly Version</a>	
<a href="#">Interactive Discussion</a>	



## 2.3 Simulation of the relationship between AOD and PM<sub>2.5</sub> by GEOS-Chem

We use the GEOS-Chem chemical transport model (version 9-01-03; <http://geos-chem.org>) to calculate the spatiotemporally resolved relationship between ground-level PM<sub>2.5</sub> and satellite-retrieved column AOD.

Our nested GEOS-Chem simulation at  $1/2^\circ \times 2/3^\circ$  spatial resolution with 47 vertical levels (14 levels in the lowest 2 km) is driven by assimilated meteorology from the Goddard Earth Observing System (GEOS-5). A global simulation at  $2^\circ \times 2.5^\circ$  spatial resolution is used to provide boundary conditions for the nested domain (Wang et al., 2004). We spin up the model for one month before each simulation to remove the effects of initial conditions on the aerosol simulation.

GEOS-Chem includes a fully coupled treatment of tropospheric oxidant-aerosol chemistry (Bey et al., 2001; Park et al., 2004). The GEOS-Chem aerosol simulation includes the sulfate-nitrate-ammonium system (Park et al., 2004; Pye et al., 2009), primary (Park et al., 2003) and secondary (Henze et al., 2006, 2008; Liao et al., 2007; Fu et al., 2008) organics, mineral dust (Fairlie et al., 2007), and sea salt (Jaegle et al., 2011). We estimate the concentration of organic matter (OM) from the simulated primary organic carbon (OC) using spatially and seasonally values from OMI (Ozone Monitoring Instrument) NO<sub>2</sub> and AMS (Aerosol Mass Spectrometer) measurements following Philip et al. (2014). Gas-aerosol phase partitioning is simulated using ISOR-ROPIA II thermodynamic scheme (Fountoukis and Nenes, 2007). GEOS-Chem calculates AOD using relative humidity dependent aerosol optical properties following Martin et al. (2003). Dust optics are from Ridley et al. (2012).

Anthropogenic emissions are based on the Multi-resolution Emission Inventory for China (MEIC; <http://www.meicmodel.org>) for 2010, and the Zhang et al. (2009) inventory for surrounding East Asia regions for 2006. Both inventories are scaled to the simulation year (2012–2013), following Ohara et al. (2007). Non-anthropogenic emissions include biomass burning emissions (GFED-3) (Mu et al., 2011), biogenic emissions (MEGAN) (Guenther et al., 2006), soil NO<sub>x</sub> (Yienger and Levy, 1995; Wang et al.,

[Title Page](#)

[Abstract](#)

[Introduction](#)

[Conclusions](#)

[References](#)

[Tables](#)

[Figures](#)

◀

▶

◀

▶

[Back](#)

[Close](#)

[Full Screen / Esc](#)

[Printer-friendly Version](#)

[Interactive Discussion](#)



Title Page

Abstract

Introduction

Conclusions

References

Tables

Figures

◀

▶

◀

▶

Back

Close

Full Screen / Esc

Printer-friendly Version

Interactive Discussion



1998), lightning NO<sub>x</sub> (Murray et al., 2012), aircraft NO<sub>x</sub> (Wang et al., 1998; Stettler et al., 2011), ship SO<sub>2</sub> from EDGAR (Olivier et al., 2001) and volcanic SO<sub>2</sub> emissions (Fischer et al., 2011). Emissions are distributed into the lower mixed layer, with a correction to the GEOS-5 predicted nighttime mixing depths and overprediction of HNO<sub>3</sub> following Heald et al. (2012) and Walker et al. (2012).

5 We apply GEOS-Chem to simulate the relationship between ground level PM<sub>2.5</sub> and column AOD, specifically PM<sub>2.5</sub>/AOD. PM<sub>2.5</sub> concentrations are calculated at 35 % relative humidity for consistency with in-situ measurements. For consistency with GOXI AOD and PM<sub>2.5</sub> ground-based measurements, we sample the simulated AOD only from 10 hours that GOXI has retrievals (00:00–07:00 UTC), and calculate the simulated daily PM<sub>2.5</sub> from 24 h averages as reported for the ground-based PM<sub>2.5</sub> measurements. The simulation period is May 2012–April 2013 as the GEOS-5 meteorological fields are not available afterward. The mismatch with observations for May–December 2013 has 15 the potential to degrade performance, but as will be shown no clear loss of quality is apparent.

## 2.4 In-situ PM<sub>2.5</sub> measurements

We collect PM<sub>2.5</sub> measurements from 494 monitors to evaluate the GOXI-derived 20 values. In-situ PM<sub>2.5</sub> daily measurements in Mainland China for 2013 are primarily from the official website of the China Environmental Monitoring Center (CEMC; <http://113.108.142:20035/emcpublish/>). Data are also collected from some provinces (e.g. Shandong, Zhejiang) and municipalities (e.g. Beijing and Tianjin) with additional sites that are not included in the CEMC website. Daily in-situ PM<sub>2.5</sub> data in northern Taiwan for 2013 are from the Taiwan Environmental Protection Administration 25 (TEPA; <http://taqm.epa.gov.tw>). The in-situ PM<sub>2.5</sub> data in both Mainland China and northern Taiwan are measured by a collection of the Tapered Element Oscillating Microbalance Methods (TEOMs) and beta-attenuation methods (BAMs) with some TEOMs being heated to 30 °C and others to 50 °C (CNAQS GB3095-2012, 2012; <http://taqm.epa.gov.tw>). The specific instrument (BAMs or TEOMs) used by each mon-

5 monitoring site is unknown. The effective relative humidity of the resultant PM<sub>2.5</sub> measurement likely varies diurnally and seasonally as a function of the ambient temperature. Semivolatile losses are expected from the TEOMs. The network design is unclear but appears to include compliance objectives that may affect monitor placement. Despite these issues, we use the monitoring data to evaluate our satellite-derived PM<sub>2.5</sub> since the monitoring data offer valuable information about ground-level PM<sub>2.5</sub> concentrations. We also collect PM<sub>2.5</sub> measurements from a monitor in Beijing measured by the Surface PARTiculate mAtter Network (SPARTAN, [www.spartan-network.org](http://www.spartan-network.org)) using a three-wavelength nephelometer and an impaction filter sampler (Snider et al., 2015). The 10 SPARTAN, CEMC and TEPA PM<sub>2.5</sub> monitoring data combined with AERONET AOD are used to estimate the empirical relationship between PM<sub>2.5</sub> and AOD, and to further evaluate the relationship simulated by the model.

## 2.5 Statistical Terms

15 Root mean square error (RMSE), mean fractional bias (MFB) and mean fractional error (MFE) are defined as

$$\text{RMSE} = \sqrt{\frac{1}{N} \sum_{i=1}^N (F_i - O_i)^2} \quad (1)$$

$$\text{MFB} = \frac{1}{N} \sum_{i=1}^N \frac{(F_i - O_i)}{\left(\frac{F_i + O_i}{2}\right)} \times 100\% \quad (2)$$

$$\text{MFE} = \frac{1}{N} \sum_{i=1}^N \frac{|F_i - O_i|}{\left(\frac{F_i + O_i}{2}\right)} \times 100\% \quad (3)$$

20 where  $F_i$  is the forecast value of the parameter in question,  $O_i$  is the corresponding observed value, and  $N$  is the number of observations.

<a href="#">Title Page</a>	<a href="#">Abstract</a>	<a href="#">Introduction</a>		
<a href="#">Conclusions</a>	<a href="#">References</a>			
<a href="#">Tables</a>	<a href="#">Figures</a>			
<a href="#">◀</a>		<a href="#">▶</a>		
<a href="#">◀</a>		<a href="#">▶</a>		
<a href="#">Back</a>	<a href="#">Close</a>			
<a href="#">Full Screen / Esc</a>				
<a href="#">Printer-friendly Version</a>				
<a href="#">Interactive Discussion</a>				



### 3 Results and discussion

#### 3.1 Evaluation of satellite AOD and the simulated relationship between $PM_{2.5}$ and AOD

Figure 1 shows the effects of our cloud-screening filters on GOCI AOD. The left panel shows GOCI true color images from 5 July 2013 at 10:30 (top) and 11:30 (bottom) Korean Standard Time. The boxes identify challenging regions with thick white cloud, dark cloud-free oceans and grey shading that appears to be thin cloud. The operational GOCI AOD retrievals, shown in the middle panel, correctly exclude thick clouds, but report high AOD for the potentially thin clouds. Although these grey regions could contain aerosol, we err on the side of caution. Application of our additional temporal and spatial cloud filters removes the suspicious pixels from the original GOCI data, as shown in the right panel. Our filters reject 10.3 % of the operational GOCI AOD data. We evaluate the cloud filters further below.

Figure 2 (top) shows monthly averages of coincident filtered hourly GOCI and AERONET AOD for January–December 2013 at combined Beijing and northern Taiwan stations. GOCI AOD is highly consistent with AERONET observations, especially at combined Beijing where RMSE is only 0.079. The reduced consistency in northern Taiwan may reflect the fewer observations there. The effect of excluding our cloud-screening filters is negligible for coincident comparisons with AERONET since AERONET is already cloud-screened. The exclusion of our cloud filters for a non-coincident comparison that includes all GOCI data would introduce significant error vs. AERONET observations, increasing MFE by a factor of 1.1–2.3 in Beijing and northern Taiwan. As will be shown, GOCI-derived  $PM_{2.5}$  offers an additional test of cloud screening filters.

We investigate the filtered diurnal variation of GOCI AOD at the above AERONET stations and find the level of AOD is uniform within a day (e.g. the coefficient of variation in Beijing is 0.1), similar to AERONET observations.

ACPD

15, 17251–17281, 2015

#### Estimating ground-level $PM_{2.5}$ in Eastern China

J. Xu et al.

[Title Page](#)

[Abstract](#)

[Introduction](#)

[Conclusions](#)

[References](#)

[Tables](#)

[Figures](#)

◀

▶

◀

▶

[Back](#)

[Close](#)

[Full Screen / Esc](#)

[Printer-friendly Version](#)

[Interactive Discussion](#)



Figure 2 (bottom) shows the relationship between the ground level PM<sub>2.5</sub> and the columnar AOD as simulated by GEOS-Chem and from ground-based measurements. The measured ratio in Beijing shows pronounced seasonal variation with values high in winter and low in spring. The measured ratio in northern Taiwan exhibits little seasonal variation. The annual mean GEOS-Chem PM<sub>2.5</sub>/AOD ratio well reproduces the ground-based measurements despite the temporal inconsistency of the two metrics for May–December. The simulation captures the pronounced seasonal variation in Beijing and the comparably aseasonal behavior in northern Taiwan. The simulated seasonal variation of PM<sub>2.5</sub>/AOD in Beijing arises from the seasonal variation of mixed layer depth (factor of 2 higher in summer than winter) combined with the near-constant columnar AOD throughout the year as shown in Fig. 1 (top).

Snider et al. (2015) interpreted coincident measurements of AOD, PM<sub>2.5</sub>, and nephelometer measurements of aerosol scattering and found that the temporal variation of the PM<sub>2.5</sub>/AOD ratio in Beijing was primarily driven by the vertical profile in aerosol scattering. We examine the seasonal variation in the simulated PM<sub>2.5</sub>/AOD and similarly find that the ratio of ground-level aerosol scattering to columnar AOD contributes most (89 %) of the monthly variability in the PM<sub>2.5</sub>/AOD ratio in Beijing.

### 3.2 Evaluation of ground-level PM<sub>2.5</sub> derived from GOCI AOD

Figure 3 shows the seasonal and annual distribution of PM<sub>2.5</sub> over eastern China at a spatial resolution of 6 km for 2013. In both GOCI-derived and measured PM<sub>2.5</sub>, winter concentrations in eastern China exceed 100  $\mu\text{g m}^{-3}$  over vast regions, with lower values in summer. Both GOCI-derived and in-situ measurements reveal that PM<sub>2.5</sub> in northern China is higher than in southern China, especially for the Beijing, Hebei and Shandong provinces where the annual PM<sub>2.5</sub> is almost 100  $\mu\text{g m}^{-3}$  or more. Prior work has attributed this regional enhancement to high emission rates (Zhao et al., 2013; Zhang et al., 2013), that in part arises from exports (Jiang et al., 2015).

Figure 4 compares annual averages of daily ground-measured PM<sub>2.5</sub> from 494 sites with coincident daily GOCI-derived PM<sub>2.5</sub> from pixels that contain the ground-based

<a href="#">Title Page</a>	
<a href="#">Abstract</a>	<a href="#">Introduction</a>
<a href="#">Conclusions</a>	<a href="#">References</a>
<a href="#">Tables</a>	<a href="#">Figures</a>
<a href="#">◀</a>	<a href="#">▶</a>
<a href="#">◀</a>	<a href="#">▶</a>
<a href="#">Back</a>	<a href="#">Close</a>
<a href="#">Full Screen / Esc</a>	
<a href="#">Printer-friendly Version</a>	
<a href="#">Interactive Discussion</a>	



sites. A significant correlation ( $r = 0.81$ ,  $N = 494$ ) with a slope near unity (1.01) is found. GOCl-derived  $\text{PM}_{2.5}$  corrects the significant underestimation of  $\text{PM}_{2.5}$  from GEOS-Chem (slope = 0.68,  $r = 0.92$ ) and achieves greater consistency than MODIS-derived  $\text{PM}_{2.5}$  with ground-based measurements (slope = 1.1,  $r = 0.78$ ).

5 Figure 5 shows monthly averages of GOCl-derived  $\text{PM}_{2.5}$  and in-situ measurements at four regions outlined in Fig. 3. Regions are selected based on the level of  $\text{PM}_{2.5}$  concentration and the population of residents. A high degree of consistency is found in all regions. Both datasets show more seasonal variation in northern regions like Beijing and Shandong than southern regions like Shanghai and northern Taiwan. Both indicate that  $\text{PM}_{2.5}$  concentrations in northern regions are generally higher than in southern regions. The exclusion of our cloud screening filters from the GOCl AOD would introduce significant bias in GOCl-derived  $\text{PM}_{2.5}$  vs. ground-based measurements especially in summer, increasing RMSE by a factor of 1.5–6.4 in Beijing ( $95.2 \mu\text{g m}^{-3}$ ), Shandong cluster ( $61.9 \mu\text{g m}^{-3}$ ), Shanghai cluster ( $29.0 \mu\text{g m}^{-3}$ ) and northern Taiwan ( $47.3 \mu\text{g m}^{-3}$ ).

### 3.3 Seasonal variation of $\text{PM}_{2.5}$

20 Figure 6 shows the monthly averages of coincident daily GOCl-derived and in-situ  $\text{PM}_{2.5}$  concentrations for the domain of eastern China. The GOCl-derived  $\text{PM}_{2.5}$  and ground-based observations both show similar seasonal variation with values high in winter and low in summer. Exclusion of our temporal and spatial cloud-screening filters from GOCl-derived  $\text{PM}_{2.5}$  would increase RMSE by a factor of 3.4. Figure 6 also shows the chemical speciation of GOCl-derived  $\text{PM}_{2.5}$ , as calculated from the GEOS-Chem simulation of  $\text{PM}_{2.5}$  fractional chemical composition applied to GOCl-derived  $\text{PM}_{2.5}$ . Aerosol water is attached to each component according to its hygroscopicity. 25 Secondary inorganic aerosols (SIA;  $\text{SO}_4^{2-}$ ,  $\text{NO}_3^-$ ,  $\text{NH}_4^+$ ) are the most abundant components throughout the year, accounting for 65 % of  $\text{PM}_{2.5}$  concentrations, followed by OM (18 %). The  $\text{NO}_3^-$  and OM concentration increases by a factor of 2 in winter,

[Title Page](#)[Abstract](#)[Introduction](#)[Conclusions](#)[References](#)[Tables](#)[Figures](#)[|◀](#)[▶|](#)[◀](#)[▶](#)[Back](#)[Close](#)[Full Screen / Esc](#)[Printer-friendly Version](#)[Interactive Discussion](#)

Estimating  
ground-level PM<sub>2.5</sub> in  
Eastern China

J. Xu et al.

[Title Page](#)[Abstract](#)[Introduction](#)[Conclusions](#)[References](#)[Tables](#)[Figures](#)[|](#)[|](#)[◀](#)[▶](#)[Back](#)[Close](#)[Full Screen / Esc](#)[Printer-friendly Version](#)[Interactive Discussion](#)

constituting the largest fraction of PM<sub>2.5</sub> (31 % for NO<sub>3</sub><sup>-</sup> and 26 % for OM). Summer is predominately controlled by SIA (74 %). Dust plays an important role in spring (15 %) and fall (15 %). Our seasonal variation of chemical composition is generally consistent with ground-based measurements in previous works across eastern China. A number

5 of studies in Beijing, the Yangtze River delta and Pearl River delta regions all reported that OM and SIA are the most important components of PM<sub>2.5</sub> through the year (He et al., 2001; Ye et al., 2003; Tao et al., 2012; Zhang et al., 2013). Zhang et al. (2008) showed consistent seasonal patterns in OM at 18 stations in China, with a winter maximum, and a summer minimum, similar to the seasonality of OM in this work. Zhang  
10 et al. (2013) studied the chemical speciation of PM<sub>2.5</sub> in Beijing and indicated the percentage of SIA in PM<sub>2.5</sub> is the largest in summer, consistent with our result.

The seasonal variation of PM<sub>2.5</sub> in Fig. 6 is driven by a combination of meteorological conditions and emissions. Summer is associated with an average mixing height in eastern China from GEOS-5 that is 1.6 times higher than in winter. The GEOS-Chem  
15 simulation reveals that the increase of OM in winter is primarily driven by biofuel emissions from burning wood, animal waste and agricultural waste (Bond et al., 2004) for heating in eastern China. The monthly variation of biofuel emissions is almost identical ( $r = 0.97$ ) with that of OM concentrations. The spatial distribution of biofuel emission is primarily north of the Yangtze River, especially from the North China Plain. The significant contribution from biofuel emissions to the OM concentration in our work is consistent with Bond et al. (2004) who found residential biofuel emissions were responsible for ~ 70 % of OC emissions in China. The increase of NO<sub>3</sub><sup>-</sup> in winter in Fig. 6 is consistent with prior attribution of the increase of NO<sub>3</sub><sup>-</sup> in winter to the favorable formation of NH<sub>4</sub>NO<sub>3</sub> at low temperatures (Wang et al., 2013).

20 Table 1 shows the annual chemical speciation of GOCl-derived PM<sub>2.5</sub> in regions outlined in Fig. 3 and in overall eastern China. SIA and OM are the most abundant species. Among the SIA components, SO<sub>4</sub><sup>2-</sup> and NO<sub>3</sub><sup>-</sup> concentrations are similar in the Beijing, Shandong and Shanghai regions, whereas in eastern China and northern Taiwan SO<sub>4</sub><sup>2-</sup> is the dominant component. OM concentrations in the Beijing and

Shandong regions are considerably higher than in the other regions, similar to or even exceeding the concentrations of  $\text{SO}_4^{2-}$  and  $\text{NO}_3^-$ . Our estimation of  $\text{PM}_{2.5}$  composition is generally consistent with in-situ measurements in prior studies. In Beijing, the concentrations of SIA in this work are similar to Zhang et al. (2013) who measured concentrations for 2009–2010 of  $13.6 \pm 12.4 \mu\text{g m}^{-3}$  for  $\text{SO}_4^{2-}$ ,  $11.3 \pm 10.8 \mu\text{g m}^{-3}$  for  $\text{NO}_3^-$  and  $6.9 \pm 7.1 \mu\text{g m}^{-3}$  for  $\text{NH}_4^+$ . Our SIA concentrations in Beijing are also comparable with Yang et al. (2011) who measured concentrations for 2005–2006 of  $15.8 \pm 10.3 \mu\text{g m}^{-3}$  for  $\text{SO}_4^{2-}$ ,  $10.1 \pm 6.09 \mu\text{g m}^{-3}$  for  $\text{NO}_3^-$  and  $7.3 \pm 4.2 \mu\text{g m}^{-3}$  for  $\text{NH}_4^+$ . The OC concentration in Beijing in this work is smaller than Zhang et al. (2013) of  $16.9 \pm 10.0 \mu\text{g m}^{-3}$  and Yang et al. (2011) of  $24.5 \pm 12.0 \mu\text{g m}^{-3}$ . In Shandong and surrounding regions, our concentrations are smaller than in Cheng et al. (2011) by a factor of about 2, perhaps related to unresolved sources. Our results in Shanghai cluster are comparable with Yang et al. (2011) for 1999–2000, except the OC concentration in this work is considerable lower than Yang et al. (2011) of  $16.8 \mu\text{g m}^{-3}$ . In northern Taiwan, our  $\text{NO}_3^-$  is similar to Fang et al. (2002) for 2001–2003, yet our estimations of  $\text{SO}_4^{2-}$  and  $\text{NH}_4^+$  are higher than Fang et al. (2002) by a factor of two, which could be driven by changes in emissions over the last decade. In summary, the chemical speciation broadly represents in-situ measurements with some location-dependent discrepancies.

### 3.4 Population exposure to ambient $\text{PM}_{2.5}$ in eastern China

We estimate the population exposure to ambient  $\text{PM}_{2.5}$  in eastern China for 2013 at a spatial resolution of 6 km using our GOCl-derived  $\text{PM}_{2.5}$  and the Gridded Population of the World (GPW; Tobler et al., 1997) data for 2010 from the Socioeconomic Data and Applications Center (GPW version 3; <http://sedac.ciesin.columbia.edu/>). Table 1 also provides the population-weighted GOCl-derived  $\text{PM}_{2.5}$  for regions outlined in Fig. 3 and for overall eastern China. The population-weighted  $\text{PM}_{2.5}$  exceeds the area-weighted for all regions except northern Taiwan and Shandong and surrounding regions. The overall population-weighted  $\text{PM}_{2.5}$  concentration for eastern China for

Title Page

Abstract

Introduction

Conclusions

References

Tables

Figures

|◀

▶|

◀

▶

Back

Close

Full Screen / Esc

Printer-friendly Version

Interactive Discussion



2013 is  $53.8 \mu\text{g m}^{-3}$ . The level of  $\text{PM}_{2.5}$  for Beijing and Shandong regions in this study is similar to Ma et al. (2014) who suggested that the  $\text{PM}_{2.5}$  concentration over the North China Plain for 2013 is  $85\text{--}95 \mu\text{g m}^{-3}$ . The  $\text{PM}_{2.5}$  concentration in eastern China in this study is also comparable with previous works. Van Donkelaar et al. (2015) estimated the  $\text{PM}_{2.5}$  concentration over eastern Asia for 2001–2010 is  $50.3 \pm 24.3 \mu\text{g m}^{-3}$ . Geng et al. (2015) estimated the  $\text{PM}_{2.5}$  concentration in China for 2006–2012 is  $71 \mu\text{g m}^{-3}$ , higher than our work. According to the World Health Organization (WHO) Air Quality Interim Target-1, an annual mean  $\text{PM}_{2.5}$  concentration of  $35 \mu\text{g m}^{-3}$  or higher is associated with about 15 % increased risk of premature mortality. As shown in Table 1, all regions in eastern China considerably exceed the Interim Target-1 level of  $\text{PM}_{2.5}$  concentration, especially in Beijing and Shandong regions where the  $\text{PM}_{2.5}$  concentration is almost triple the Interim Target-1 level. These elevated concentrations threaten the health of the 603 million inhabitants (Table 1) of eastern China.

## 4 Conclusions

We estimated the ground-level concentration of  $\text{PM}_{2.5}$  in eastern China for 2013 using AOD retrieved from GOHI satellite instrument, coupled with the relationship of AOD to  $\text{PM}_{2.5}$  simulated by a global chemical transport model (GEOS-Chem). GOHI-derived  $\text{PM}_{2.5}$  was compared with in-situ measurements throughout eastern China.

We applied a set of filters to GOHI AOD to remove cloud contamination. The filtered GOHI AOD showed significant agreement with AERONET AOD at Beijing and northern Taiwan (MFB of  $-1.2$  to  $6.7\%$ ). We also evaluated the simulated relationship of  $\text{PM}_{2.5}$  and AOD from GEOS-Chem by using an empirical relationship calculated from nearly collocated ground-based  $\text{PM}_{2.5}$  monitors and AERONET AOD stations. A high degree of consistency was observed between the GEOS-Chem simulation and ground-based measurements with MFB of  $-0.52$  to  $8.0\%$ .

<a href="#">Title Page</a>	
<a href="#">Abstract</a>	<a href="#">Introduction</a>
<a href="#">Conclusions</a>	<a href="#">References</a>
<a href="#">Tables</a>	<a href="#">Figures</a>
<a href="#">◀</a>	<a href="#">▶</a>
<a href="#">◀</a>	<a href="#">▶</a>
<a href="#">Back</a>	<a href="#">Close</a>
<a href="#">Full Screen / Esc</a>	
<a href="#">Printer-friendly Version</a>	
<a href="#">Interactive Discussion</a>	



The GOCl-derived PM<sub>2.5</sub> were highly consistent with in-situ measurements, capturing the similar seasonal and spatial distribution throughout the eastern China. The highest PM<sub>2.5</sub> concentrations were found in winter over northern regions. The annual averages of GOCl-derived PM<sub>2.5</sub> were significantly correlated (0.81) with surface measurements with a slope near unity (1.01). Monthly comparison of GOCl-derived PM<sub>2.5</sub> with ground-based measurements across the entire region of eastern China was also in good agreement with RMSE = 13.1  $\mu\text{g m}^{-3}$ . The exclusion of our cloud-screening filters in GOCl retrievals would introduce significant bias in GOCl-derived PM<sub>2.5</sub>, especially in summer and would increase the RMSE by a factor of 1.5–6.4.

The chemical speciation of GOCl-derived PM<sub>2.5</sub> revealed that secondary inorganic aerosols (SIA; SO<sub>4</sub><sup>2-</sup>, NO<sub>3</sub><sup>-</sup>, NH<sub>4</sub><sup>+</sup>) and organic matter (OM) dominated throughout the year. Nitrate had a winter maximum due to aerosol thermodynamics. OM increased by a factor of 2 in winter, which was primarily driven by biofuel emission for heating in northern China. Dust played an important role in spring and fall.

The population-weighted GOCl-derived PM<sub>2.5</sub> for 2013 at 6 km resolution in eastern China was 53.8  $\mu\text{g m}^{-3}$ , suggesting ~ 600 million people in China live in regions with PM<sub>2.5</sub> concentrations exceeding the suggested 35  $\mu\text{g m}^{-3}$  by the World Health Organization (WHO) Air Quality Interim Target-1, of which 130 million people in Beijing and Shandong regions are seriously threatened by even higher PM<sub>2.5</sub> concentrations.

Population-weighted PM<sub>2.5</sub> of pixels containing ground-based monitors is much higher at 82.4  $\mu\text{g m}^{-3}$ , suggesting the value of the newly established PM<sub>2.5</sub> network to monitor these seriously polluted regions.

The satellite measurements of AOD from the GOCl instrument coupled with the relationship between AOD and PM<sub>2.5</sub> simulated by a chemical transport model have the potential to provide a unique synopsis of ground-level PM<sub>2.5</sub> concentrations at fine spatial resolution in the most polluted and populated part of China. Development of this capability will depend on both the quality of GOCl aerosol products and the aerosol simulation. Assimilating satellite observations of trace gases from the forthcoming GEMS

<a href="#">Title Page</a>	
<a href="#">Abstract</a>	<a href="#">Introduction</a>
<a href="#">Conclusions</a>	<a href="#">References</a>
<a href="#">Tables</a>	<a href="#">Figures</a>
<a href="#">◀</a>	<a href="#">▶</a>
<a href="#">◀</a>	<a href="#">▶</a>
<a href="#">Back</a>	<a href="#">Close</a>
<a href="#">Full Screen / Esc</a>	
<a href="#">Printer-friendly Version</a>	
<a href="#">Interactive Discussion</a>	



(Geostationary Environment Spectrometer) geostationary platform would provide additional constraints on  $PM_{2.5}$  composition.

*Acknowledgements.* We are grateful to the GOXI, AERONET, CEMC, TEPA and SPARTAN for providing available data used in this study. Funding for this work was provided by NSERC (Natural Sciences and Engineering Research Council of Canada) and by an Izaak Walton Killam Memorial Scholarship for J. Xu. Computational facilities are partially provided by ACEnet, the regional high performance computing consortium for universities in Atlantic Canada.

## References

Bey, I., Jacob, D. J., Yantosca, R. M., Logan, J. A., Field, B. D., Fiore, A. M., Li, Q. B., Liu, H. G. Y., Mickley, L. J., and Schultz, M. G.: Global modeling of tropospheric chemistry with assimilated meteorology: model description and evaluation, *J. Geophys. Res.*, 106, 23073–23095, doi:10.1029/2001JD000807, 2001.

Bond, T. C., Streets, D. G., Yarber, K. F., Nelson, S. M., Woo, J.-H., and Klimont, Z.: A technology-based global inventory of black and organic carbon emissions from combustion, *J. Geophys. Res.*, 109, D14203, doi:10.1029/2003JD003697, 2004.

Boys, B. L., Martin, R. V., van Donkelaar, A., MacDonell, R. J., Hsu, N. C., Cooper, M. J., Yantosca, R. M., Lu, Z., Streets, D. G., Zhang, Q., and Wang, S. W.: Fifteen-year global time series of satellite-derived fine particulate matter, *Environ. Sci. Technol.*, 48, 11109–11118, 2014.

Cheng, S., Yang, L. X., Zhou, X., Wang, Z., Zhou, Y., Gao, X., Nie, W., Wang, X., Xu, P., and Wang, W.: Evaluating  $PM_{2.5}$  ionic components and source apportionment in Jinan, China from 2004 to 2008 using trajectory statistical methods, *J. Environ. Monitor.*, 13, 1662–1671, 2011.

Cho, Y. and Youn, H.: Characteristics of COMS Meteorological Imager, in: Sensors, Systems, and Next-Generation Satellites X, Proc. SPIE, Stockholm, Sweden, doi:10.1117/12.688393, 2006.

Fairlie, D. T., Jacob, D. J., and Park, R. J.: The impact of transpacific transport of mineral dust in the United States, *Atmos. Environ.*, 41, 1251–1266, doi:10.1016/j.atmosenv.2006.09.048, 2007.

[Title Page](#)

[Abstract](#)

[Introduction](#)

[Conclusions](#)

[References](#)

[Tables](#)

[Figures](#)

◀

▶

[Back](#)

[Close](#)

[Full Screen / Esc](#)

[Printer-friendly Version](#)

[Interactive Discussion](#)



Estimating  
ground-level PM<sub>2.5</sub> in  
Eastern China

J. Xu et al.

Title Page

Abstract

Introduction

Conclusions

References

Tables

Figures

|

|

|

|

Back

Close

Full Screen / Esc

Printer-friendly Version

Interactive Discussion



Fang, G., Chang, C., Wu, Y., Fu, P. P., Yang, C., Chen, C., and Chang, S.: Ambient suspended particulate matters and related chemical species study in central Taiwan, Taichung during 1998–2001, *Atmos. Environ.*, 36, 1921–1928, 2002.

Fischer, J. A., Jacob, D. J., Wang, Q., Bahreini, R., Carouge, C. C., Cubison, M. J., Dibb, J. E., Diehl, T., Jimenez, J. L., and Leibensperger, E. M.: Sources, distribution, and acidity of sulfate–ammonium aerosol in the Arctic in winter–spring, *Atmos. Environ.*, 45, 7301–7318, 2011.

Fountoukis, C. and Nenes, A.: ISORROPIA II: a computationally efficient thermodynamic equilibrium model for K<sup>+</sup>–Ca<sup>2+</sup>–Mg<sup>2+</sup>–NH<sub>4</sub><sup>+</sup>–Na<sup>+</sup>–SO<sub>4</sub><sup>2-</sup>–NO<sub>3</sub><sup>-</sup>–Cl<sup>-</sup>–H<sub>2</sub>O aerosols, *Atmos. Chem. Phys.*, 7, 4639–4659, doi:10.5194/acp-7-4639-2007, 2007.

Fu, T., Jacob, D. J., Witrock, F., Burrows, J. P., Vrekoussis, M., and Henze, D. K.: Global budgets of atmospheric glyoxal and methylglyoxal, and implications for formation of secondary organic aerosols, *J. Geophys. Res.*, 113, D15303, doi:10.1029/2007JD009505, 2008.

Geng, G., Zhang, Q., Martin, R. V., van Donkelaar, A., Huo, H., Che, H., Lin, J., and He, K.: Estimating long-term PM<sub>2.5</sub> concentrations in China using satellite-based aerosol optical depth and a chemical transport model, *Remote Sens. Environ.*, in press, 2015.

Goldberg, M.: A systematic review of the relation between long-term exposure to ambient air pollution and chronic diseases, *Rev. Environ. Health*, 23, 243, doi:10.1515/REVEH.2008.23.4.243, 2008.

Guenther, A., Karl, T., Harley, P., Wiedinmyer, C., Palmer, P. I., and Geron, C.: Estimates of global terrestrial isoprene emissions using MEGAN (Model of Emissions of Gases and Aerosols from Nature), *Atmos. Chem. Phys.*, 6, 3181–3210, doi:10.5194/acp-6-3181-2006, 2006.

He, K., Yang, F., Ma, Y., Zhang, Q., Yao, X., Chan, C. K., Cadle, S., Chan, T., and Mulawa, P.: The characteristics of PM<sub>2.5</sub> in Beijing, China, *Atmos. Environ.*, 35, 4959, doi:10.1016/S1352-2310(01)00301-6, 2001.

Heald, C. L., Collett Jr., J. L., Lee, T., Benedict, K. B., Schwandner, F. M., Li, Y., Clarisse, L., Hurtmans, D. R., Van Damme, M., Clerbaux, C., Coheur, P.-F., Philip, S., Martin, R. V., and Pye, H. O. T.: Atmospheric ammonia and particulate inorganic nitrogen over the United States, *Atmos. Chem. Phys.*, 12, 10295–10312, doi:10.5194/acp-12-10295-2012, 2012.

Henze, D. K. and Seinfeld, J. H.: Global secondary organic aerosol from isoprene oxidation, *Geophys. Res. Lett.*, 33, L09812, doi:10.1029/2006GL025976, 2006.

Henze, D. K., Seinfeld, J. H., Ng, N. L., Kroll, J. H., Fu, T.-M., Jacob, D. J., and Heald, C. L.: Global modeling of secondary organic aerosol formation from aromatic hydrocarbons: high- vs. low-yield pathways, *Atmos. Chem. Phys.*, 8, 2405–2420, doi:10.5194/acp-8-2405-2008, 2008.

5 Holben, B., Eck, T., Slutsker, I., Tanre, D., Buis, J., Setzer, A., Vermote, E., Reagan, J., Kaufman, Y., and Nakajima, T.: AERONET – a federated instrument network and data archive for aerosol characterization, *Remote Sens. Environ.*, 66, 1–16, 1998.

10 Holben, B., Tanre, D., Smirnov, A., Eck, T., Slutsker, I., Abuhassan, N., Newcomb, W., Schafer, J., Chatenet, B., and Lavenu, F.: An emerging ground-based aerosol climatology: aerosol optical depth from AERONET, *J. Geophys. Res.*, 106, 12067–12097, 2001.

Hu, X., Waller, L. A., Al-Hamdan, M. Z., Crosson, W. L., Estes Jr., M. G., Estes, S. M., Quattrochi, D. A., Sarnat, J. A., and Liu, Y.: Estimating ground-level PM<sub>2.5</sub> concentrations in the southeastern US using geographically weighted regression, *Environ. Res.*, 121, 1–10, 2013.

15 Hyer, E. J., Reid, J. S., and Zhang, J.: An over-land aerosol optical depth data set for data assimilation by filtering, correction, and aggregation of MODIS Collection 5 optical depth retrievals, *Atmos. Meas. Tech.*, 4, 379–408, doi:10.5194/amt-4-379-2011, 2011.

Jaeglé, L., Quinn, P. K., Bates, T. S., Alexander, B., and Lin, J.-T.: Global distribution of sea salt aerosols: new constraints from in situ and remote sensing observations, *Atmos. Chem. Phys.*, 11, 3137–3157, doi:10.5194/acp-11-3137-2011, 2011.

20 Jiang, X., Zhang, Q., Zhao, H., Geng, G., Peng, L., Guan, D., Kan, H., Huo, H., Lin, J., Brauer, M., Martin, R. V., and He, K.: Revealing the hidden health costs embodied in Chinese exports, *Environ. Sci. Technol.*, 49, 4381–4388, doi:10.1021/es506121s, 2015.

25 Kang, G., Youn, H. S., Choi, S. B., and Coste, P.: Radiometric calibration of COMS geostationary ocean color imager, *IEEE T. Geosci. Remote*, 6361, 636112, doi:10.1111/12.689888, 2006.

Kloog, I., Nordio, F., Coull, B. A., and Schwartz, J.: Incorporating local land use regression and satellite aerosol optical depth in a hybrid model of spatiotemporal PM<sub>2.5</sub> exposures in the Mid-Atlantic states, *Environ. Sci. Technol.*, 46, 11913–11921, 2012.

30 Laden, F., Schwartz, J., Speizer, F. E., and Dockery, D. W.: Reduction in fine particulate air pollution and mortality: extended follow-up of the Harvard Six Cities study, *Am. J. Resp. Crit. Care*, 173, 667–672, 2006.

[Title Page](#)

[Abstract](#)

[Introduction](#)

[Conclusions](#)

[References](#)

[Tables](#)

[Figures](#)

◀

▶

◀

▶

[Back](#)

[Close](#)

[Full Screen / Esc](#)

[Printer-friendly Version](#)

[Interactive Discussion](#)



Lee, J., Kim, J., Song, C. H., Ryu, J., Ahn, Y., and Song, C. K.: Algorithm for retrieval of aerosol optical properties over the ocean from the Geostationary Ocean Color Imager, *Remote Sens. Environ.*, 114, 1077, doi:10.1016/j.rse.2009.12.021, 2010.

5 Lee, J., Kim, J., Yang, P., and Hsu, N. C.: Improvement of aerosol optical depth retrieval from MODIS spectral reflectance over the global ocean using new aerosol models archived from AERONET inversion data and tri-axial ellipsoidal dust database, *Atmos. Chem. Phys.*, 12, 7087–7102, doi:10.5194/acp-12-7087-2012, 2012.

10 Liao, H., Henze, D. K., Seinfeld, J. H., Wu, S., and Mickley, L. J.: Biogenic secondary organic aerosol over the United States: comparison of climatological simulations with observations, *J. Geophys. Res.*, 112, D06201, doi:10.1029/2006JD007813, 2007.

15 Lim, S. S., Vos, T., Flaxman, A. D., Danaei, G., Shibuya, K., Adair-Rohani, H., AlMazroa, M. A., Amann, M., Anderson, H. R., Andrews, K. G., Aryee, M., Atkinson, C., Bacchus, L. J., Bahlam, A. N., Balakrishnan, K., Balmes, J., Barker-Collo, S., Baxter, A., Bell, M. L., Blore, J. D., Blyth, F., Bonner, C., Borges, G., Bourne, R., Boussinesq, M., Brauer, M., Brooks, P., Bruce, N. G., Brunekreef, B., Bryan-Hancock, C., Bucello, C., Buchbinder, R., Bull, F., Burnett, R. T., Byers, T. E., Calabria, B., Carapetis, J., Carnahan, E., Chafe, Z., Charlson, F., Chen, H., Chen, J. S., Cheng, A. T., Child, J. C., Cohen, A., Colson, K. E., Cowie, B. C., Darby, S., Darling, S., Davis, A., Degenhardt, L., Dentener, F., Des Jarlais, D. C., Devries, K., Dherani, M., Ding, E. L., Dorsey, E. R., Driscoll, T., Edmond, K., Ali, S. E., Engell, R. E., Erwin, P. J., Fahimi, S., Falder, G., Farzadfar, F., Ferrari, A., Finucane, M. M., Flaxman, S., Fowkes, F. G. R., Freedman, G., Freeman, M. K., Gakidou, E., Ghosh, S., Giovannucci, E., Gmel, G., Graham, K., Grainger, R., Grant, B., Gunnell, D., Gutierrez, H. R., Hall, W., Hoek, H. W., Hogan, A., Hosgood III, H. D., Hoy, D., Hu, H., Hubbell, B. J., Hutchings, S. J., Ibeanusi, S. E., Jacklyn, G. L., Jasrasaria, R., Jonas, J. B., Kan, H., Kanis, J. A., Kassebaum, N., Kawakami, N., Khang, Y., Khatibzadeh, S., Khoo, J., Kok, C., Laden, F., Lal-loo, R., Lan, Q., Lathlean, T., Leasher, J. L., Leigh, J., Li, Y., Lin, J. K., Lipshultz, S. E., London, S., Lozano, R., Lu, Y., Mak, J., Malekzadeh, R., Mallinger, L., Marcenes, W., March, L., Marks, R., Martin, R., McGale, P., McGrath, J., Mehta, S., Memish, Z. A., Mensah, G. A., Merriman, T. R., Micha, R., Michaud, C., Mishra, V., Hanafiah, K. M., Mokdad, A. A., Morawska, L., Mozaffarian, D., Murphy, T., Naghavi, M., Neal, B., Nelson, P. K., Nolla, J. M., Norman, R., Olives, C., Omer, S. B., Orchard, J., Osborne, R., Ostro, B., Page, A., Pandey, K. D., Parry, C. D., Passmore, E., Patra, J., Pearce, N., Pelizzari, P. M., Petzold, M., Phillips, M. R., Pope, D., Pope III, C. A., Powles, J., Rao, M., Razavi, H., Re-

[Title Page](#)

[Abstract](#)

[Introduction](#)

[Conclusions](#)

[References](#)

[Tables](#)

[Figures](#)

◀

▶

◀

▶

[Back](#)

[Close](#)

[Full Screen / Esc](#)

[Printer-friendly Version](#)

[Interactive Discussion](#)



## Estimating ground-level PM<sub>2.5</sub> in Eastern China

J. Xu et al.

hfuess, E. A., Rehm, J. T., Ritz, B., Rivara, F. P., Roberts, T., Robinson, C., Rodriguez-Portales, J. A., Romieu, I., Room, R., Rosenfeld, L. C., Roy, A., Rushton, L., Salomon, J. A., Sampson, U., Sanchez-Riera, L., Sanman, E., Sapkota, A., Seedat, S., Shi, P., Shield, K., Shivakoti, R., Singh, G. M., Sleet, D. A., Smith, E., Smith, K. R., Stapelberg, N. J., Steenland, K., Stöckl, H., Stovner, L. J., Straif, K., Straney, L., Thurston, G. D., Tran, J. H., Van Dingenen, R., van Donkelaar, A., Veerman, J. L., Vijayakumar, L., Weintraub, R., Weissman, M. M., White, R. A., Whiteford, H., Wiersma, S. T., Wilkinson, J. D., Williams, H. C., Williams, W., Wilson, N., Woolf, A. D., Yip, P., Zielinski, J. M., Lopez, A. D., Murray, C. J., and Ezzati, M.: A comparative risk assessment of burden of disease and injury attributable to 67 risk factors and risk factor clusters in 21 regions, 1990–2010: a systematic analysis for the Global Burden of Disease Study 2010, *Lancet*, 380, 2224–2260, doi:10.1016/S0140-6736(12)61766-8, 2012.

Liu, Y., Park, R. J., Jacob, D. J., Li, Q., Kilaru, V., and Sarnat, J. A.: Mapping annual mean ground-level PM<sub>2.5</sub> concentrations using Multiangle Imaging Spectroradiometer aerosol optical thickness over the contiguous United States, *J. Geophys. Res.*, 109, D22206, doi:10.1029/2004JD005025, 2004.

Liu, Y., Paciorek, C. J., and Koutrakis, P.: Estimating regional spatial and temporal variability of PM<sub>2.5</sub> concentrations using satellite data, meteorology, and land use information, *Environ. Health Persp.*, 117, 886–892, 2009.

Ma, Z., Hu, X., Huang, L., Bi, J., and Liu, Y.: Estimating ground-level PM<sub>2.5</sub> in China using satellite remote sensing, *Environ. Sci. Technol.*, 48, 7436–7444, 2014.

Martin, R. V., Jacob, D. J., Yantosca, R. M., Chin, M., and Ginoux, P.: Global and regional decreases in tropospheric oxidants from photochemical effects of aerosols, *J. Geophys. Res.*, 108, 4097, doi:10.1029/2002JD002622, 2003.

Ministry of Environmental Protection of the People's Republic of China: Chinese National Ambient Air Quality Standard, CNAQS, Beijing, GB3095-2012, 2012.

Mu, M., Randerson, J., Van der Werf, G., Giglio, L., Kasibhatla, P., Morton, D., Collatz, G., DeFries, R., Hyer, E., and Prins, E.: Daily and 3 hourly variability in global fire emissions and consequences for atmospheric model predictions of carbon monoxide, *J. Geophys. Res.*, 116, 1–19, 2011.

Murray, L. T., Jacob, D. J., Logan, J. A., Hudman, R. C., and Koshak, W. J.: Optimized regional and interannual variability of lightning in a global chemical transport model constrained by LIS/OTD satellite data, *J. Geophys. Res.*, 117, D20307, doi:10.1029/2012JD017934, 2012.

<a href="#">Title Page</a>	<a href="#">Abstract</a>	<a href="#">Introduction</a>
<a href="#">Conclusions</a>	<a href="#">References</a>	
<a href="#">Tables</a>	<a href="#">Figures</a>	
<a href="#">◀</a>	<a href="#">▶</a>	
<a href="#">◀</a>	<a href="#">▶</a>	
<a href="#">Back</a>	<a href="#">Close</a>	
<a href="#">Full Screen / Esc</a>		
	<a href="#">Printer-friendly Version</a>	
	<a href="#">Interactive Discussion</a>	



Estimating  
ground-level PM<sub>2.5</sub> in  
Eastern China

J. Xu et al.

[Title Page](#)[Abstract](#)[Introduction](#)[Conclusions](#)[References](#)[Tables](#)[Figures](#)[|](#)[|](#)[◀](#)[▶](#)[Back](#)[Close](#)[Full Screen / Esc](#)[Printer-friendly Version](#)[Interactive Discussion](#)

Ohara, T., Akimoto, H., Kurokawa, J., Horii, N., Yamaji, K., Yan, X., and Hayasaka, T.: An Asian emission inventory of anthropogenic emission sources for the period 1980–2020, *Atmos. Chem. Phys.*, 7, 4419–4444, doi:10.5194/acp-7-4419-2007, 2007.

Olivier, J. G. J. and Berdowski, J. J. M.: Global emissions sources and sinks, in: *The Climate System*, edited by: Berdowski, J., Guicherit, R., and Heij, B. J., A. A. Balkema Publishers/Swets & Zeitlinger Publishers, Lisse, the Netherlands, 33–78, 2001.

Park, M. E., Song, C. H., Park, R. S., Lee, J., Kim, J., Lee, S., Woo, J.-H., Carmichael, G. R., Eck, T. F., Holben, B. N., Lee, S.-S., Song, C. K., and Hong, Y. D.: New approach to monitor transboundary particulate pollution over Northeast Asia, *Atmos. Chem. Phys.*, 14, 659–674, doi:10.5194/acp-14-659-2014, 2014.

Park, R. J., Jacob, D. J., Chin, M., and Martin, R. V.: Sources of carbonaceous aerosols over the United States and implications for natural visibility, *J. Geophys. Res.*, 108, 4355, doi:10.1029/2002JD003190, 2003.

Park, R. J., Jacob, D. J., Field, B. D., Yantosca, R. M., and Chin, M.: Natural and transboundary pollution influences on sulfate-nitrate-ammonium aerosols in the United States: implications for policy, *J. Geophys. Res.*, 109, D15204, doi:10.1029/2003JD004473, 2004.

Philip, S., Martin, R. V., Pierce, J. R., Jimenez, J. L., Zhang, Q., Canagaratna, M. R., Spracklen, D. V., Nowlan, C. R., Lamsal, L. N., Cooper, M. J., and Krotkov, N. A.: Spatially and seasonally resolved estimate of the ratio of global organic matter to organic carbon, *Atmos. Environ.*, 87, 34, doi:10.1016/j.atmosenv.2013.11.065, 2014.

Pye, H. O. T., Liao, H., Wu, S., Mickley, L. J., Jacob, D. J., Henze, D. K., and Seinfeld, J. H.: Effect of changes in climate and emissions on future sulfate-nitrate-ammonium aerosol levels in the United States, *J. Geophys. Res.*, 114, D01205, doi:10.1029/2008JD010701, 2009.

Ridley, D. A., Heald, C. L., and Ford, B.: North African dust export and deposition: a satellite and model perspective., *J. Geophys. Res.*, 117, D02202, doi:10.1029/2011JD016794, 2012.

Silva, R. A., West, J. J., Zhang, Y., Anenberg, S. C., Lamarque, J., Shindell, D. T., Collins, W. J., Dalsoren, S., Faluvegi, G., and Folberth, G.: Global premature mortality due to anthropogenic outdoor air pollution and the contribution of past climate change, *Environ. Res. Lett.*, 8, 034005, doi:10.1088/1748-9326/8/3/034005, 2013.

Smirnov, A., Holben, B., Eck, T., Dubovik, O., and Slutsker, I.: Cloud-screening and quality control algorithms for the AERONET database, *Remote Sens. Environ.*, 73, 337–349, 2000.

Snider, G., Weagle, C. L., Martin, R. V., van Donkelaar, A., Conrad, K., Cunningham, D., Gordon, C., Zwicker, M., Akoshile, C., Artaxo, P., Anh, N. X., Brook, J., Dong, J., Garland, R. M.,

## Estimating ground-level $\text{PM}_{2.5}$ in Eastern China

J. Xu et al.

[Title Page](#)

[Abstract](#)

[Introduction](#)

[Conclusions](#)

[References](#)

[Tables](#)

[Figures](#)

◀

▶

[Back](#)

[Close](#)

[Full Screen / Esc](#)

[Printer-friendly Version](#)

[Interactive Discussion](#)



Estimating  
ground-level PM<sub>2.5</sub> in  
Eastern China

J. Xu et al.

[Title Page](#)[Abstract](#)[Introduction](#)[Conclusions](#)[References](#)[Tables](#)[Figures](#)[|](#)[|](#)[◀](#)[▶](#)[Back](#)[Close](#)[Full Screen / Esc](#)[Printer-friendly Version](#)[Interactive Discussion](#)

Wang, Y., McElroy, M. B., Jacob, D. J., and Yantosca, R. M.: A nested grid formulation for chemical transport over Asia: applications to CO, *J. Geophys. Res.*, 109, 27, doi:10.1029/2004JD005237, 2004.

5 Wang, Y., Zhang, Q. Q., He, K., Zhang, Q., and Chai, L.: Sulfate-nitrate-ammonium aerosols over China: response to 2000–2015 emission changes of sulfur dioxide, nitrogen oxides, and ammonia, *Atmos. Chem. Phys.*, 13, 2635–2652, doi:10.5194/acp-13-2635-2013, 2013.

WHO (World Health Organization, 2005): Air Quality Guidelines Global Update 2005, WHO/Europe, Copenhagen, Denmark, 2006.

10 Yang, F., Tan, J., Zhao, Q., Du, Z., He, K., Ma, Y., Duan, F., Chen, G., and Zhao, Q.: Characteristics of PM<sub>2.5</sub> speciation in representative megacities and across China, *Atmos. Chem. Phys.*, 11, 5207–5219, doi:10.5194/acp-11-5207-2011, 2011.

Ye, B., Ji, X., Yang, H., Yao, X., Chan, C. K., Cadle, S. H., Chan, T., and Mulawa, P. A.: Concentration and chemical composition of PM<sub>2.5</sub> in Shanghai for a 1 year period, *Atmos. Environ.*, 37, 499, doi:10.1016/S1352-2310(02)00918-4, 2003.

15 Yienger, J. and Levy, H.: Empirical model of global soil-biogenic NO<sub>x</sub> emissions, *J. Geophys. Res.*, 100, 11447–11464, 1995.

Zhang, Q., Streets, D. G., Carmichael, G. R., He, K. B., Huo, H., Kannari, A., Klimont, Z., Park, I. S., Reddy, S., Fu, J. S., Chen, D., Duan, L., Lei, Y., Wang, L. T., and Yao, Z. L.: Asian emissions in 2006 for the NASA INTEX-B mission, *Atmos. Chem. Phys.*, 9, 5131–5153, doi:10.5194/acp-9-5131-2009, 2009.

20 Zhang, R., Jing, J., Tao, J., Hsu, S.-C., Wang, G., Cao, J., Lee, C. S. L., Zhu, L., Chen, Z., Zhao, Y., and Shen, Z.: Chemical characterization and source apportionment of PM<sub>2.5</sub> in Beijing: seasonal perspective, *Atmos. Chem. Phys.*, 13, 7053–7074, doi:10.5194/acp-13-7053-2013, 2013.

25 Zhang, X. Y., Wang, Y. Q., Zhang, X. C., Guo, W., and Gong, S. L.: Carbonaceous aerosol composition over various regions of China during 2006, *J. Geophys. Res.*, 113, D14111, doi:10.1029/2007JD009525, 2008.

30 Zhao, P. S., Dong, F., He, D., Zhao, X. J., Zhang, X. L., Zhang, W. Z., Yao, Q., and Liu, H. Y.: Characteristics of concentrations and chemical compositions for PM<sub>2.5</sub> in the region of Beijing, Tianjin, and Hebei, China, *Atmos. Chem. Phys.*, 13, 4631–4644, doi:10.5194/acp-13-4631-2013, 2013.

Estimating  
ground-level PM<sub>2.5</sub> in  
Eastern China

J. Xu et al.

**Table 1.** Annual PM<sub>2.5</sub> concentrations, chemical speciation and population in regions outlined in Fig. 3 and in overall eastern China (including Beijing and surrounding region, Shandong province, Shanghai and surrounding region) for 2013. Aerosol water is not associated with each PM<sub>2.5</sub> component for consistency with measurement protocols. PM<sub>2.5</sub> concentration is at 35 % of relative humidity.

Region	Beijing	Shandong	Shanghai	Eastern China	Northern Taiwan
Population-weighted GOCl-derived PM <sub>2.5</sub> (µg m <sup>-3</sup> )	90.8	89.1	56.9	53.8	18.9
Area-weighted GOCl-derived PM <sub>2.5</sub> (µg m <sup>-3</sup> )	86.5	89.1	51.0	44.3	23.6
SO <sub>4</sub> <sup>2-</sup> (µg m <sup>-3</sup> )	12.8	14.0	9.2	13.1	5.1
NO <sub>3</sub> <sup>-</sup> (µg m <sup>-3</sup> )	14.5	16.1	8.5	4.2	2.1
NH <sub>4</sub> <sup>+</sup> (µg m <sup>-3</sup> )	8.9	9.8	5.7	3.3	2.2
OC (µg m <sup>-3</sup> )	10.3	9.6	4.3	2.9	1.6
BC (µg m <sup>-3</sup> )	6.3	5.2	2.6	1.6	0.8
Dust (µg m <sup>-3</sup> )	9.1	8.3	4.9	4.4	2.9
Sea Salt (µg m <sup>-3</sup> )	0.2	0.4	0.9	1.9	2.2
OM (µg m <sup>-3</sup> )	17.1	15.7	7.4	5.4	3.0
Population (million people)	37.8	91.8	109.0	603.3	15.8

<a href="#">Title Page</a>	<a href="#">Abstract</a>	<a href="#">Introduction</a>
<a href="#">Conclusions</a>	<a href="#">References</a>	
<a href="#">Tables</a>	<a href="#">Figures</a>	
<a href="#">◀</a>	<a href="#">▶</a>	
<a href="#">◀</a>	<a href="#">▶</a>	
<a href="#">Back</a>	<a href="#">Close</a>	
<a href="#">Full Screen / Esc</a>		
<a href="#">Printer-friendly Version</a>		
<a href="#">Interactive Discussion</a>		



## Estimating ground-level PM<sub>2.5</sub> in Eastern China

J. Xu et al.

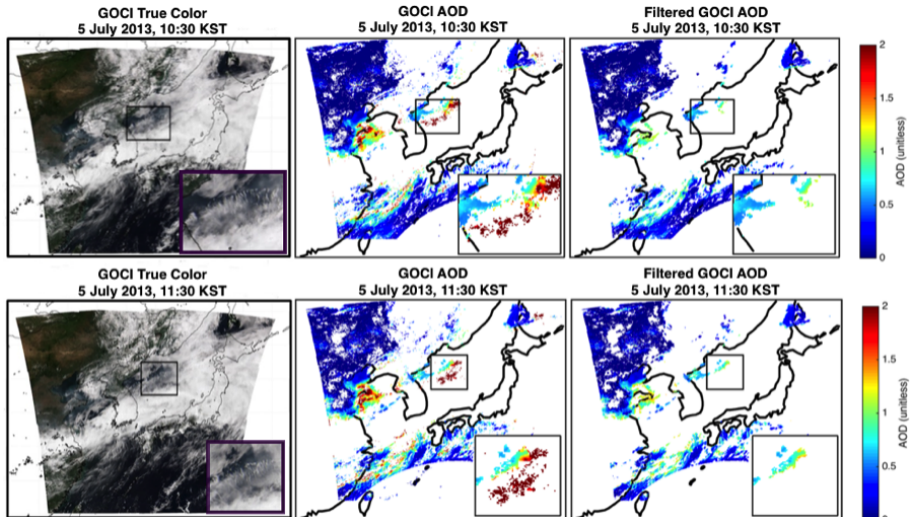


**Figure 1.** The GOCI granules from 5 July 2013, 10:30 (top) and 11:30 (bottom) Korean Standard Time. From left to right on each panel are the GOCI true color images, the operational AOD retrievals and the AOD retrievals after applying temporal and textual filters to reduce cloud contamination. The boxes highlight examples of challenging cloud fields, and are enlarged within the lower right subplot of each panel.

[Title Page](#)

[Abstract](#)

[Introduction](#)

[Conclusions](#)

[References](#)

[Tables](#)

[Figures](#)

◀

▶

[Back](#)

[Close](#)

[Full Screen / Esc](#)

[Printer-friendly Version](#)

[Interactive Discussion](#)

## Estimating ground-level $\text{PM}_{2.5}$ in Eastern China

J. Xu et al.

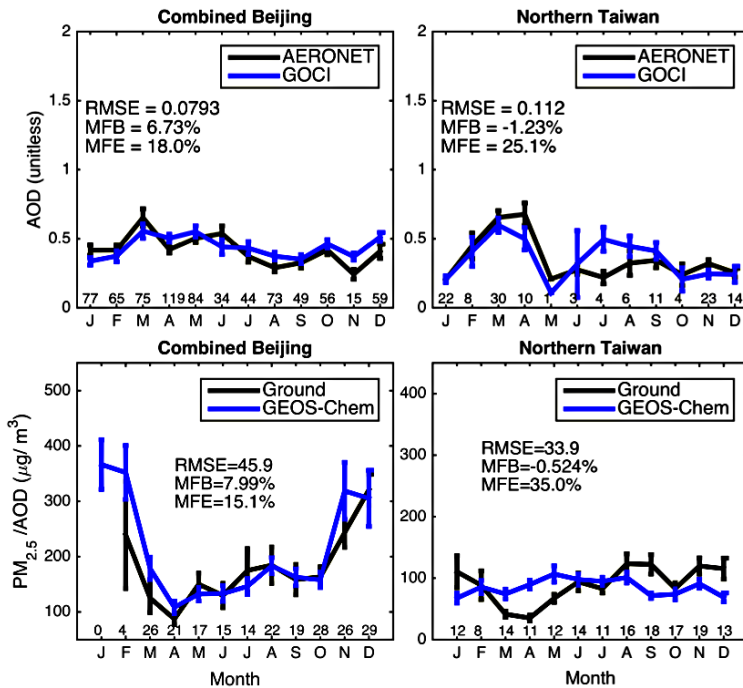


**Figure 2.** Top: Monthly time series of AOD from AERONET and GOFCI for January–December 2013. Numbers above the x axis denote the number of coincident hourly observations in each month. Bottom: Monthly averages of  $\text{PM}_{2.5}/\text{AOD}$  from ground measurements and the GEOS-Chem model simulation at AERONET sites. The ground-based ratio is sampled from daily ground  $\text{PM}_{2.5}$  coincident with AERONET AOD for January–December 2013. The GEOS-Chem simulation is for May 2012–April 2013, noncoincident with the ground-based ratio for May–December 2013. Numbers above the x axis denote the number of daily ground observations in each month. Error bars represent standard errors. RMSE, MFB and MFE are root mean square error, mean fractional bias and mean fractional error, respectively.

Estimating  
ground-level  $\text{PM}_{2.5}$  in  
Eastern China

J. Xu et al.

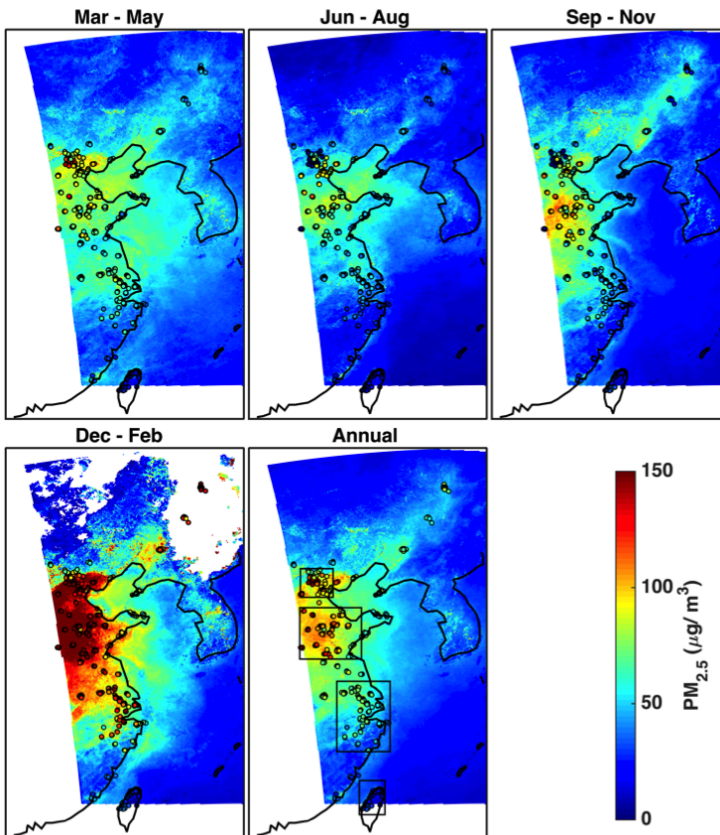


**Figure 3.** Seasonal and annual distribution of  $\text{PM}_{2.5}$  concentrations at 6 km resolution over eastern China for 2013. The background color indicates averages of GOFCI-derived daily surface  $\text{PM}_{2.5}$  concentrations. Filled circles represent averages of daily ground measurements of  $\text{PM}_{2.5}$ . Boxes in the annual map denote regions used for monthly comparisons in Fig. 5 from top to bottom: Beijing and surrounding areas, Shandong and surrounding regions, Shanghai and surrounding areas and northern Taiwan.

[Title Page](#)[Abstract](#)[Introduction](#)[Conclusions](#)[References](#)[Tables](#)[Figures](#)[|◀](#)[▶|](#)[◀](#)[▶](#)[Back](#)[Close](#)[Full Screen / Esc](#)

Estimating  
ground-level PM<sub>2.5</sub> in  
Eastern China

J. Xu et al.

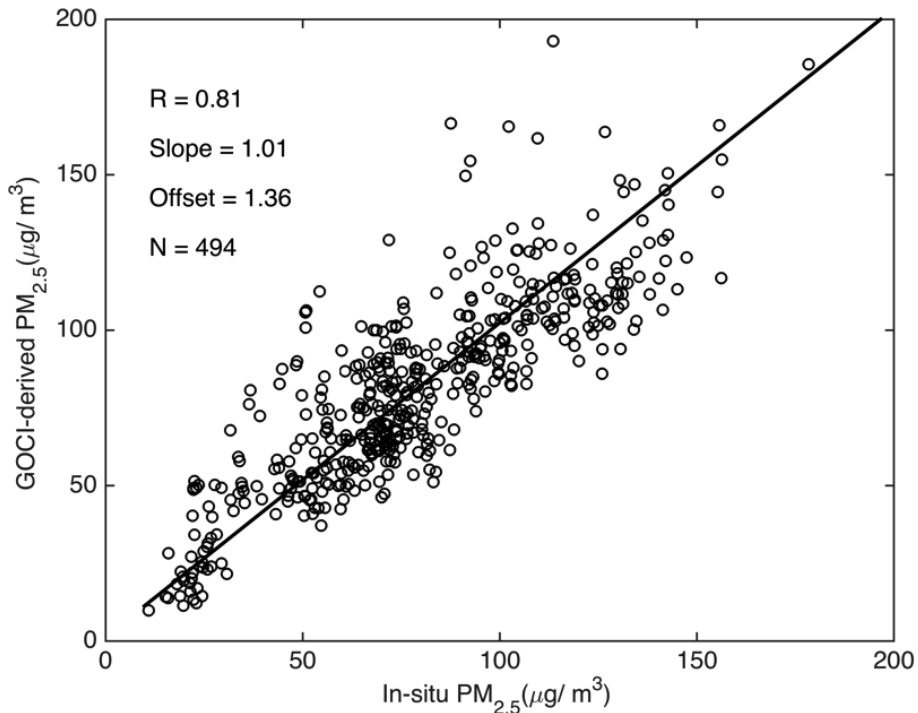


**Figure 4.** Scatterplot of the annual mean GOCl-derived PM<sub>2.5</sub> for 2013 against the annual mean PM<sub>2.5</sub> from 494 ground monitors over the GOCl domain in eastern China.

## Estimating ground-level $\text{PM}_{2.5}$ in Eastern China

J. Xu et al.

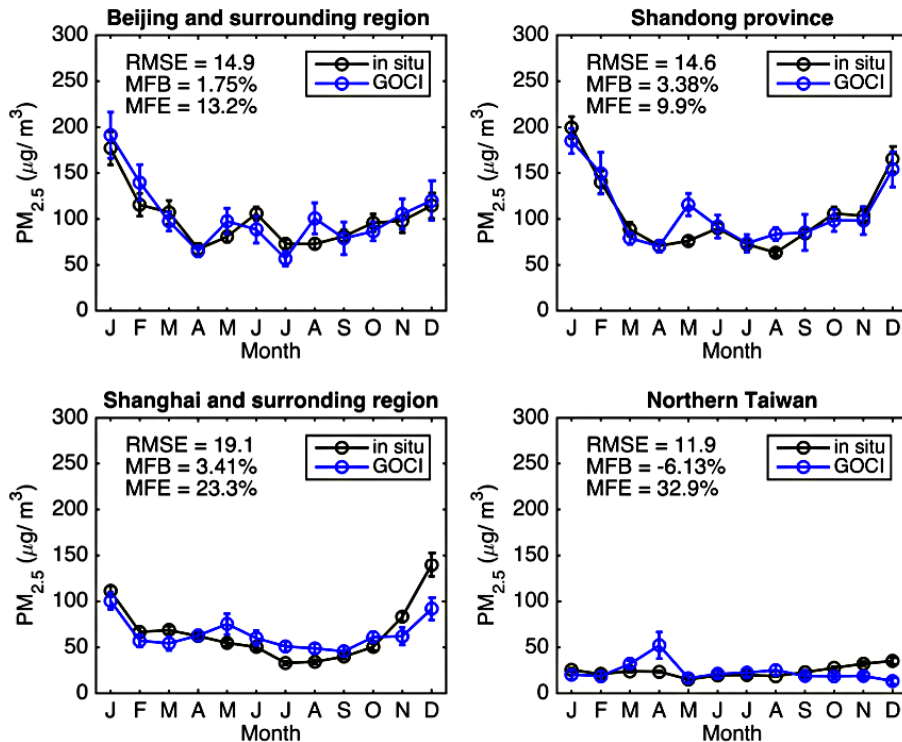


**Figure 5.** Monthly averages of daily  $\text{PM}_{2.5}$  from in-situ measurements and daily  $\text{PM}_{2.5}$  estimated from GOCI AOD for 2013. Regions are defined in Fig. 3. Error bars represent standard errors. RMSE, MFB and MFE are root mean square error, mean fractional bias and mean fractional error, respectively.

Estimating  
ground-level  $\text{PM}_{2.5}$  in  
Eastern China

J. Xu et al.

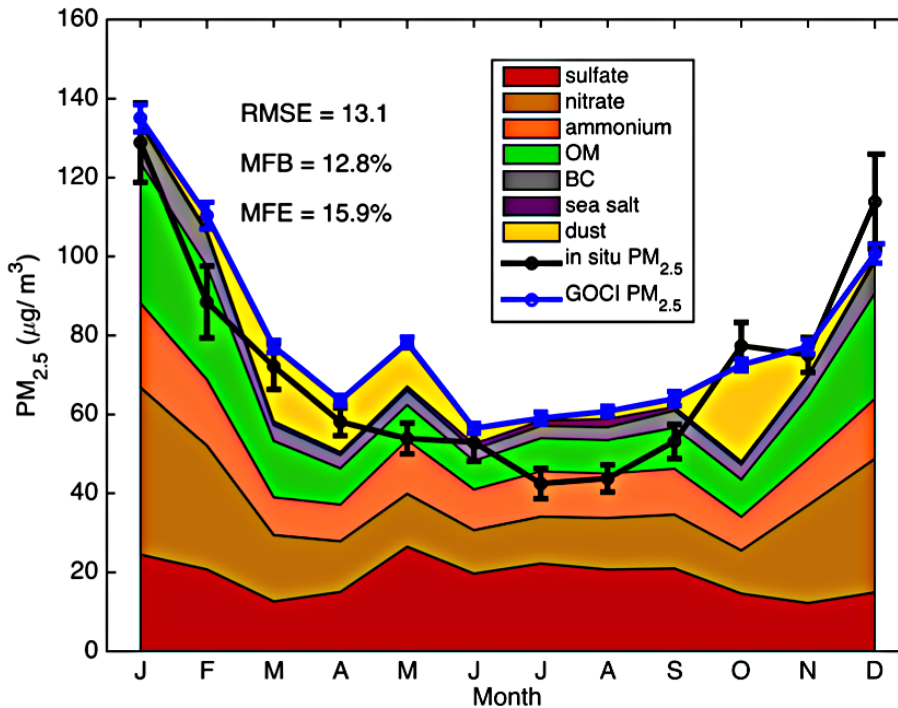


**Figure 6.** Monthly variation of GOCl-derived PM<sub>2.5</sub> and in-situ PM<sub>2.5</sub> for 2013 over eastern China, with chemical speciation for GOCl-derived PM<sub>2.5</sub>. The in-situ PM<sub>2.5</sub> is determined from the averages of all ground stations in eastern China for 2013 and GOCl-derived PM<sub>2.5</sub> is calculated from the average of all grid boxes that contain PM<sub>2.5</sub> ground monitors. The chemical speciation is calculated from the GEOS-Chem simulation of PM<sub>2.5</sub> fractional chemical composition applied to GOCl-derived PM<sub>2.5</sub>. Aerosol water is associated with each PM<sub>2.5</sub> component according to its hygroscopicity. Error bars represent standard errors.